

An Integrated Method for the Geometric Inspection of Wind Turbine Hubs with Industrial Robot



Emanuele Lindo Secco¹, Christian Deters², Helge A. Wurdemann², Hak-Keung Lam², Kaspar Althoefler²

¹Department of Mathematics & Computer Science, Liverpool Hope University, UK

²Centre of Robotics Research, Department of Informatics

King's College London, UK

seccoe@hope.ac.uk, christian.deters@kcl.ac.uk, helge.wurdemann@kcl.ac.uk, hak-keung.lam@kcl.ac.uk, kaspar.althoefler@kcl.ac.uk

ABSTRACT: Wind turbine manufacturing requires the assembly of large mechanical components, which is crucial to inspect along the production line in order to prevent high repair costs afterwards. A critical component in this process is the turbine hub, which supports the wind blades and ball bearings allowing the pitch motion. At present, hub inspection is a manual task, which requires expert operators and long execution time. This paper proposes a novel methodology for the self-adaptive inspection of wind turbine hubs via industrial robots: a set of Critical-To-Quality parameters (CTQs), are inferred from the CAD drawing of wind turbine hub; registration between robot and hub is performed; finally a CAD2robot trajectories planning is accomplished. Methodology is implemented through a Matlab and Simulink Programming Language and combined with an Industrial PC-based control technology Beckhoff TwinCAT 3. Tests with an Fanuc Industrial M-6iB robot arm and R-30iA controller have been successfully performed on re-scaled model of the hub. The flexibility of this methodology allows applications on other industrial contexts, which can benefit from automation.

Keywords: Self-adaptive Manufacturing, Geometric Inspection, Trajectory Planning, Assembly Robot, Wind Turbine Manufacturing, Real-time Automation Technology

Received: 18 October 2015, Revised 20 November 2015, Accepted 29 November 2015

© 2016 DLINE. All Rights Reserved

1. Introduction

The market of renewable energy is growing because of increasing reliability of their plants: particularly, the usage of wind turbines is expanding world widely [1,2], allowing installation of turbines even in harsh environments as it is the case of the offshore platforms. The manufacturing process of these systems requires the design and assembly of large mechanical components up to weight of tens of tons, up to length of 50÷75 m, and huge rotor diameter [3,4]. Hence, it is compulsory to guarantee that such large components, which are traveling within the factory from one manufacturing cell to another, do not have to be rejected along the construction process, because of any mechanical fault. An accurate *geometric inspection* can prevent assembly faults and highly cost for reparations afterwards.

A critical component of the wind turbine - which requires delicate inspection because of its particular geometry and task - is the turbine hub: this element embeds the hydraulic actuators - allowing pitch movements of the blades, according to the speed of the wind - and a set of ball bearing supporting these movements (Figure 1). Since the wind blades can be up to 75 m long, the geometry tolerances and mechanical quality of the hub are quite demanding to prevent catastrophic faults. Above all, the flatness of the hub flanges, supporting the bearings, has to be accurately examined before assembling the blades on top of the plant.

Geometric Inspection approaches and tools

At present, the geometric inspection of wind turbine hubs is manually performed, requires expert personnel and long execution time to complete the task [5]. Nevertheless, automatic, or semi-automatic, processes performing geometric inspection of large mechanical components do exist, based on commercial Gantry Measuring Machine [6,7], optical-based architectures and laser scanner [8]; if the inspected objects are rescaled to dimensions which are compatible with tool workspace, passive and instrumented arms - equipped with proper scanners – maybe also used [9]; moreover, a considerable effort has been done on intelligent image processing algorithms based on surface recognition [10] and laser triangulation sensors [11]. Conversely, the use of active robotic devices for the automation of the manufacturing process is quite common, due to robot movement quality and precision, as well as cost reduction in large scale production and high reproducibility [12]. On the other hand, some other applications and robotic technical solutions are quite cost demanding and require exclusive equipment while reducing the effective manufacturing flexibility.

This paper aims at combining the advantages of using a robotic device in wind turbine industry with further benefits of performing flexible and self-adaptive manufacturing. A novel hardware and software architecture is proposed for the geometric inspection of wind turbine hubs, which is inherently self-adaptive and reconfigurable. The architecture is based on a 3 stages process:

1. Critical-To-Quality (CTQ) parameters are inferred from the CAD drawing of the hub component;
2. An industrial robot is calibrated vs. the component geometry;
3. CAD2robot trajectories are automatically inferred according to motion strategy defined from selected set of CTQs.

The paper is organized in further four sessions: the first one introduces the materials and methods of the geometric inspection process, including the identification of the CTQs and calibration process; the second session details the algorithm for the self-adaptive trajectory planning according to selected CTQs to be inspected. Finally, the last two sessions present results and discussion, respectively.

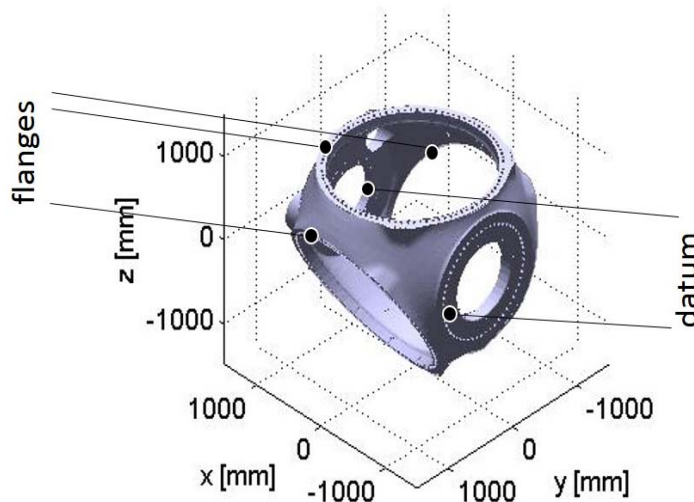


Figure 1. 3D plot of wind turbine hub (source file provided by Gamesa Corporation)

2. Geometric Inspection

In general, to perform a quality inspection of a mechanical element, it is required to define:

- ✓ A set of Critical-To-Quality parameters (CTQs) - or Geometrical Features (GFs) - which have to be measured on the component and compared with the nominal dimension of its design;
- ✓ The deviations which is allowed between the two measurements within given tolerances.

To perform a self-adaptive geometric inspection, the following hardware and software set-up is envisaged: a 3D scanning device or laser scanner is mounted on top of the end-effector of an industrial robot, while robot performing well-defined motions of the device along the large-scale hub; thanks to known kinematics of the robot, the scanning device acquires local

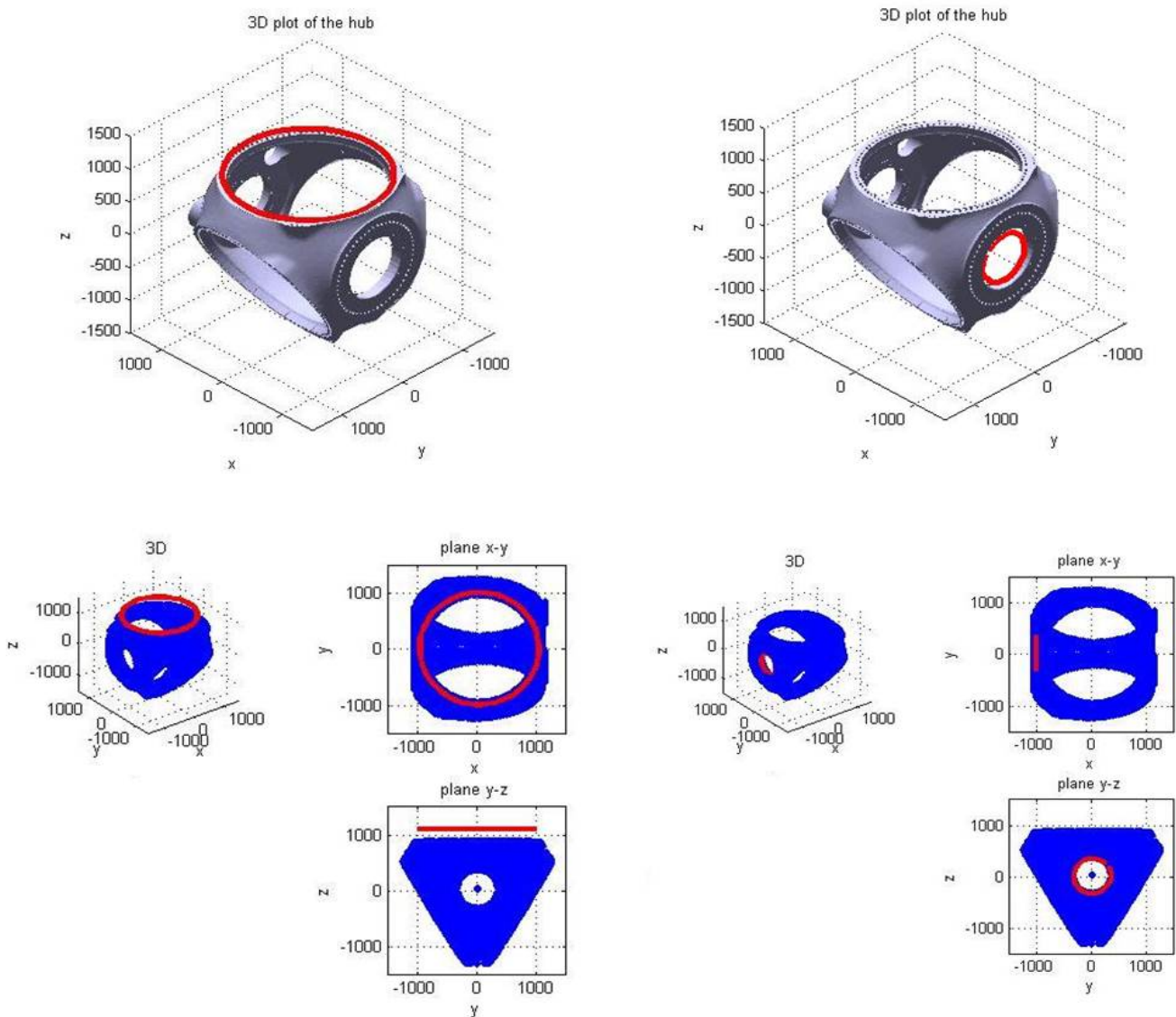


Figure 2. On top panels: 3D plot of wind turbine hub and robot trajectories for geometric inspection (red colour) of CTQ n. 5, blade flatness (left panel) and CTQ n. 8, blade angularity relative to datum (right panel) – see Table 1 and Figure 1. Bottom panels: projections of the robot trajectories on the x-y and y-z planes

geometric information of the component, so that discrete scans can be stored and mapped to the corresponding locations of the scanner and the shape of the object can be finally reconstructed. According to this scenario, the inspection task is performed with the following steps:

- **CAD2 Robot Motion** – Robot controller plans and executes trajectories of the scanner to explore areas of hub CTQs and validate - at the end the process - given tolerances. The trajectory planner receives input data from the design or CAD drawings of the component: positions and orientations of the component are extracted from the drawing and converted into robot coordinate system. From this data, the different positions to which the 3D scanner is taken to, by the industrial robot, are calculated.

- **Registration** – Reference system of the robot arm is registered with respect to reference system of the hub; homogeneous mapping between the two references is established by moving the arm to homologous points of the object and of the drawing. Local reference system of the 3D scanner is referred to the same reference systems.

- **Geometric Inspection** – 3D scanner is taken by the robot to the areas of interest where CTQs have been defined. For each robot pose (i.e. position and orientation), scanner acquires point clouds of the geometry of the part. Point clouds captured on the different poses are referred to the same object reference system thanks to robot kinematics. 3D image is reconstructed and finally, measured point clouds are compared with nominal values.

2.1 Critical-To-Quality Parameters (CTQs)

To inspect wind turbine hubs, CTQs have to be defined, according to the mechanical requirements and specifications of the component. Measurements need a set of reference surfaces or datum to be validated the geometric measurements vs. their references (Figure 1). Table I defines set of CTQs, which include:

- Position and flatness of hub flanges¹;
- Blades position and angularity;
- Holes orthogonality;
- Flanges position;
- Holes concentricity.

Because of hub symmetry (Figure 1), some CTQs are replicated along component circular structure; therefore - without loss of generality - the process may focus on a restricted number of CTQs - handling with a singular flange and wind blade – and then be easily generalized to the other ones (i.e. the whole set of CTQs).

Consistent with these criteria, four CTQs are analyzed - namely n. 5, 8, 11 and 14 of Table 1 – in order to perform the geometric inspection. For each CTQ, a suitable motion strategy of the robot-scanner system has to be defined aimed at properly inspecting the targeted GF.

2.2 Robot Motion Strategy

According to each CTQ, a motion strategy of the robot is defined to inspect areas of interest of the selected CTQ: the resultant end-effector or scanner patterns are reported in Figure 2; to inspect CTQ n. 5, namely the flatness of the blade, the robot has to perform a circular movement on top of the flange, while maintaining a constant distance – or offset - from its surface (Figure 2, left panel). The object-robot distance depends on the optical parameters of the scanner and on the precision requirements up to the precision specifications of the robot, in order to finally guarantee a proper tessellation of the surfaces and therefore a correct 3D reconstruction. Secondly, to optimize the scan, orientation of the robot tool and, therefore, of the scanner Field of View (FoV), the device has to be constantly perpendicular to the flange surface. A similar set of patterns of the robot positions and orientations can be defined for each of the other 3 CTQs: Figure 2 reports the motion strategy related to validation of CTQ n. 8 (angularity of the blade, relative to the datum).

¹The circular and flat surfaces, which are housing the bearing and supporting blades pitch regulation around their longitudinal axis

GFs	
Class	Description
1	Position of main flange holes regarding to datum E
2	Position of Pitch A regarding to datum DA
3	Position of Pitch B regarding to datum DB
4	Position of Pitch C regarding to datum DC
5	Flatness for blade A
6	Flatness for blade B
7	Flatness for blade C
8	Angularity for blade A regarding to datum E
9	Angularity for blade B regarding to datum E
10	Angularity for blade C regarding to datum E
11	Position of blade A holes regarding to datum DA
12	Position of blade B (holes regarding to datum DB
13	Position of blade C holes regarding to datum DC
14	Position of Blade A regarding to datum E
15	Position of Blade B regarding to datum E
16	Position of Blade C regarding to datum E
17	Concentricity of diameter regarding to datum E
18	Angularity between blade A and blade B
19	Angularity between blade A and blade C
20	Flatness for Main Flange
21	Perpendicularity of Pitch A hole regarding to datum A
22	Perpendicularity of Pitch A hole regarding to datum B
23	Perpendicularity of Pitch A hole regarding to datum C
24	Position of spinner flange holes regarding to datum E

Table 1. Critical To Quality parameters (CTQs) of wind turbine hub (Figure 1)

2.3 Hub-Like Component (HLC)

Wind turbine hubs are massive components, up to tens of tons of weight with volume of some cube meters. Such physical and geometric characteristics usually entail the usage of cranes and huge tools to perform the assembly, tighten the bearings and move and gather the different components during the manufacturing process.

For practical reason, in order to test the proposed methodology, a rescaled model of the wind turbine hub – namely a Hub-Like Component (HLC) - has been designed and used. The HLC has been conceived to maintain and preserve the main geometrical characteristics and CTQs of the real hub, while allowing performing geometric inspection in a laboratory environment.

A design of the HLC has been developed, which is made of two surfaces, a flange and a datum, with a relative angular displacement of 88° , as it is the case of some real wind turbine hubs. Each surface has an extension of 0.80×0.80 m. On the main surface, a flange – like hole of 0.50 m diameter is manufactured and surrounded by 8 holes of 2.5 cm diameter for tightening $8 \times M24$ bolts and nuts supporting ball bearing of the blade. On the other surface, a datum – like hole of 0.40 m diameter is inserted.

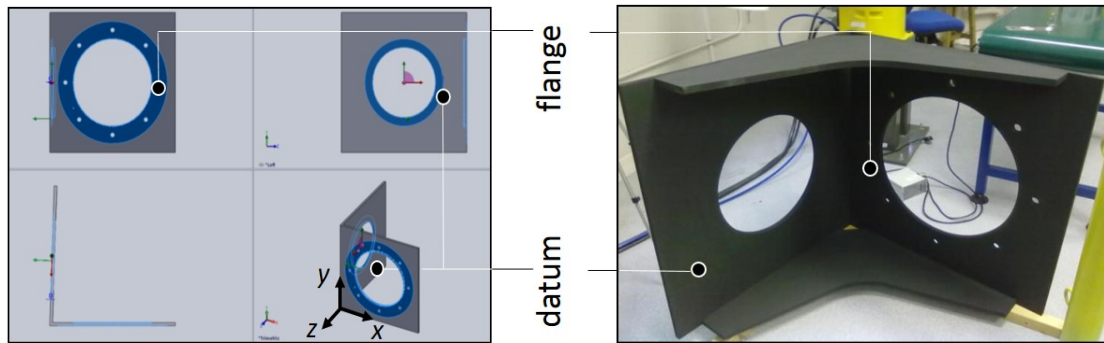


Figure 3. Design and manufacturing of the re-scaled Hub-Like Component (HLC) - left and right panels, respectively. The HLC is designed (Figure 3, left panel), and manufactured with Medium-Density Fibreboard material (MDF). Figure 3 reports the design and manufactured object (left and right panels, respectively).

2.4 Reference Systems, Flange & Datum

In order to perform robotic inspection of the HLC, a reference system which is in common between the object and the robot is set. The reference - i.e. the triplet of vectors which are anchored to the HLC flange (x, y, z) - are defined as it is shown in Figure 3, left panel (see the bottom right sub-plot).

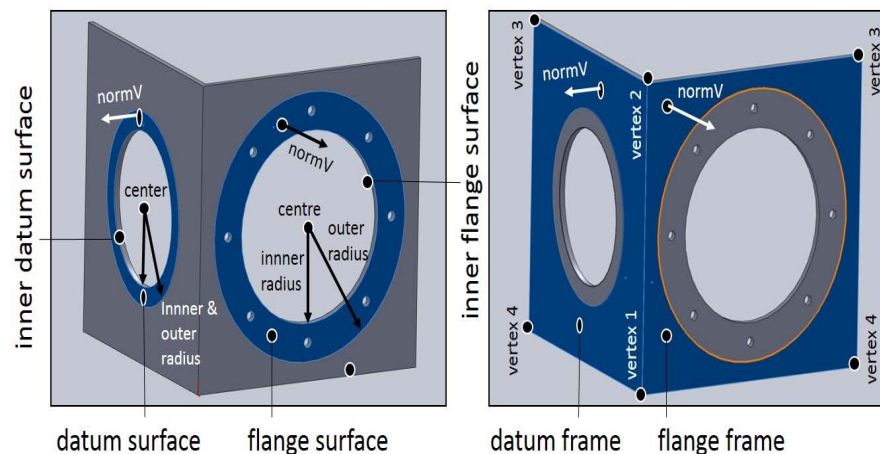


Figure 4. Geometric parameters, outer and inner surfaces (left panel) and frames (right panel) of the HLC flange and datum. Because of the CTQs characteristics and the robot motion strategy (see par. 2, subpar. 2.1 and 2.2), the inspection of the HLC requires the exploration of the flange and the datum, namely of external and internal surfaces, which have been highlighted in blue color in the design of Figure 4 (see the left panel). The marked surfaces are delimited by edges and, precisely, by:

- ✓ An external and two internal edges defining outer and inner surfaces of flange and including, respectively, the edges of the 8 holes receiving the M24 bolts and nuts of the ball bearing (Figure 4, left panel);
- ✓ An external edge and two internal edges circumscribing the outer and inner surfaces of the datum, respectively (Figure 4, left panel).

2.5 Flange & Datum Parametrization

Performing inspection of these surfaces in a self-adaptive manner requires that CTQs are parameterized and interpreted by the trajectory planning architecture later on (i.e. the *CAD2robot motion*). According to the references of Figure 4, the following parameters are defined:

- Position of the surfaces regarding the reference system, namely inner and outer radius and center of circles

constraining the flange and datum surfaces (Figure 4, left panel, blue colored parts);

- Surfaces' orientation vs. the reference system, namely triplets of components of unitary vector perpendicular to the surfaces ($normV$ in in the same figure);

- Position and orientation vector ($normV$) of vertexes, defining the flange and datum frames.

Parameters are extracted from CAD drawing and registered within structured Excel® (Microsoft Corp.) or Comma Separated Values (CSV) file format, as it is shown in Table 2.

2.6 Robot and HLC Registration

An M-6iB Industrial Robot and R-30iA Controller (by Fanuc) have been used to perform the HLC geometric inspection. The M-6iB device is an industrial 6 d.o.f. (degree of freedom) robot with a reach of 1.373 m, a global payload at wrist of 6 Kg and a position repeatability of ± 0.08 mm [13]. This hardware set up was adopted since it was available in the laboratory infrastructure and it is well representative of a typical robot equipment in a manufacturing industrial environment.

To perform the robot-HLC registration, a dial test indicator and customized support have been used: an indicator, model Baty CL1, with 0.01 mm resolution, has been attached to the robot flange by means of a support made of thermoplastic Acrylonitrile Butadiene Styrene (Figure 5). The support has been designed with SolidWorks software (by Dassault Systèmes Corp.) and manufactured with a ProJet HD3000 (by Print It 3D Ltd). Design of the support has been conceived to simultaneously safeguard:

- ✓ The mechanical alignment of the indicator, with respect to the centre of robot flange (which represents the origin of robot reference system, i.e. the tool reference system);

- ✓ The orthogonality of the orientation of the tool regarding to the flange (i.e. the z-axis of the tool reference system). These simple choices make straightforward definition of geometric offset between the tool reference system and robot default reference system (namely the one which is assigned from the controller).

To ensure an optimal positioning of the HLC component vs. robot workspace and therefore a proper reachability of HLC flange and datum surfaces, the experimental set-up of the work cell has been previously simulated with RoboGuide Simulation Software & Animation Tool (Fanuc Corp.). An overview of the virtual reality environment and of the real set-up is reported in Figure 6 (left and right panels, respectively).

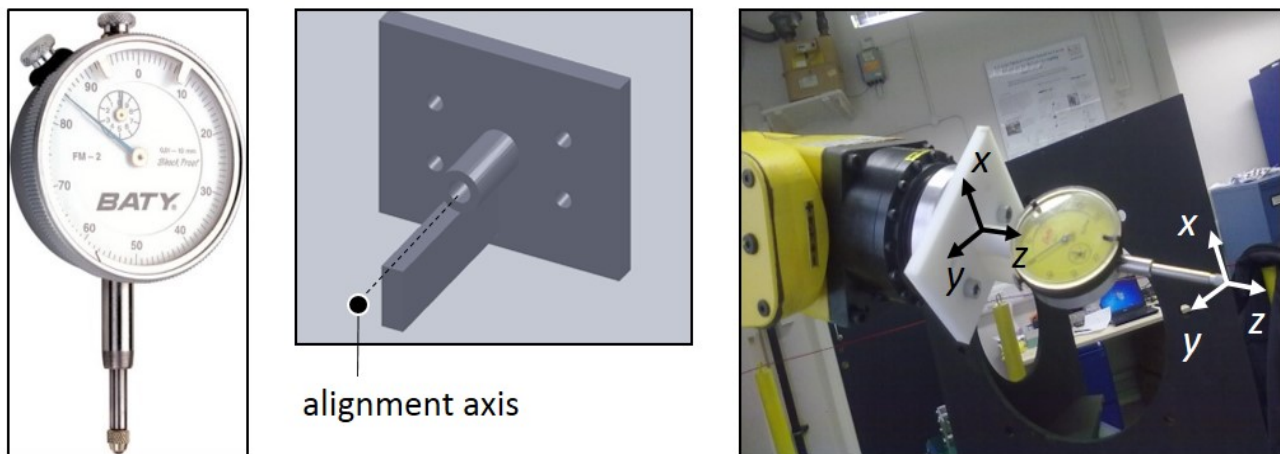


Figure 5. The robot-HLC registration set-up: a Baty CL1 dial test indicator (left panel) is mounted on the end-effector flange of Fanuc M6-iB Robot Arm (right panel) by means of an ABS customized support (central panel)

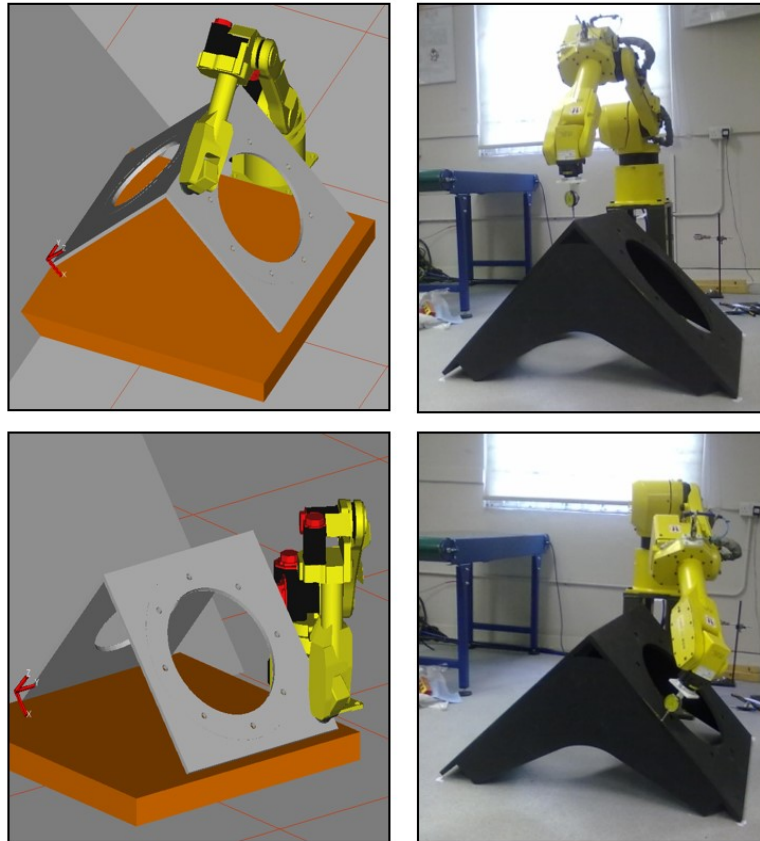


Figure 6. Simulated and experimental registration performed with Fanuc RoboGuide Software & Animation Tool (left panel) and real Fanuc M6-iB robot arm (right panel)

A typical industrial 3-point calibration procedure is implemented to register the tool and robot reference system vs. the HLC object: origin, x -axis direction and x - y plane of user reference system are assigned to the robot controller by making tip of the indicator touching the HLC surface on 3 points (Figure 6, right panels). A proper choice of the points set is chosen to have the robot frame coincident with the HLC reference system (par. 2, subpar. 2.4 and Figure 3, left panel). Registration errors are in the range between 0.25 and 0.39 mm, as a consequence of MDF surface roughness.

3. Trajectories Planning

The trajectory planning of robot is designed around the HLC. The planning has to process the CTQs objectives and interpret information into robot motions, according to strategies of Session 2, subparagraph B. Such progression is performed in 3 steps:

- **Stage 1:** A geometry to trajectory software (geom2trj) is implemented to process HLP geometric inputs (par. 2, subpar. 2.5 and Table 2) with Matlab Programming Language (Mathworks Inc.). The software returns set of trajectories parameterized in function of the scanner optical properties, according to motion strategies (par. 2, subpar. 2.2);

- **Stage 2:** A trajectory to PLC model (trj2plc) is developed with Simulink Model-Based design language (Mathworks Inc.): output data of stage 1 are sent to Fanuc robot controller in terms of poses of the robot. Programmable Logic Controller (PLC) system - interfaced with robot arm controller and real-time executing Matlab and Simulink codes within an industrial PC – is used;

- **Stage 3:** Finally, PLC to execution local program (plc2scan) is implemented within robot controller to assign positions and orientations to internal registers and execute the movements.

The following subparagraphs detail these stages.

surface	radius		center			normV		
	inner	outer	X	Y	Z	X	Y	Z
	[m]					[module = 1]		
flange	0.25	0.35	0.4	0.4	0	0	0	1
datum	0.2	0.25	0.014	0.4	-0.399	-0.999	0	-0.035

frame		point			normV		
		x	y	z	x	y	z
		[m]			[module = 1]		
flange	vertex n. 1	0	0	0	0	0	1
	vertex n. 2	0	0.8	0	0	0	1
	vertex n. 3	0.8	0.8	0	0	0	1
	vertex n. 4	0.8	0	0	0	0	1
datum	vertex n. 1	0	0	0	-0.999	0	-0.035
	vertex n. 2	0	0.8	0	-0.999	0	-0.035
	vertex n. 3	0.0279	0.8	-0.7995	-0.999	0	-0.035
	vertex n. 4	0.0279	0	-0.7995	-0.999	0	-0.035

Table 2. Geometric parameters of surfaces and frames of the HLC datum and flange (Figure 4)

3.1 Stage 1, geom2trj

Geom2trj processes Table 2 parameters vs. Figure 3 reference system and returns outputs with 4 precision digits. Finally HLC geometry, with inner and outer surfaces, and main frames of flange and datum, is reconstructed (Figure 7, left panel).

A single laser beam cannot explore all the surfaces of interest in one go. Hence, to cover the whole HLC surfaces and provide a proper optical tessellation, the robot arm motion is decomposed into multiple sub-movements, where each movement is constrained by initial and final knots [14]. Hence, a functional definition of trajectories' parameters, which modulate the density of the scan grid, is given through three parameters:

- Angular step (angStep) occurring between two consecutive knots of movement;
- Orthogonal distance (offSet) between robot end-effector tip (i.e. the plane of scanner CCD) and HLC surface (requiring end-effector orientation to be perpendicular to the explored surface).

Exploration trajectories occur out of the object or directly above the flanges, whereas other CTQs necessitate the exploration of inner surfaces; hence, trajectories are clustered into two groups:

- Explorations of the HLC surfaces at constant distance, which is defined as offset surface (surfOffset);
- Exploration of the HLC holes at constant distance from the hole inner surface, which is defined as within-hole offset (inOffset).

Finally trajectories planning are parametrized and Figure 7 (right panel) shows a set of them as obtained from geom2trj software by assuming angStep, surfOffset and inOffset equal to 0.2 rad (~11.4°), 0.2 m and 0.1 m, respectively: a constant distance of 20 cm from the surface (reported in green colour) is assumed. After the trajectories calculation, the geom2trj software:

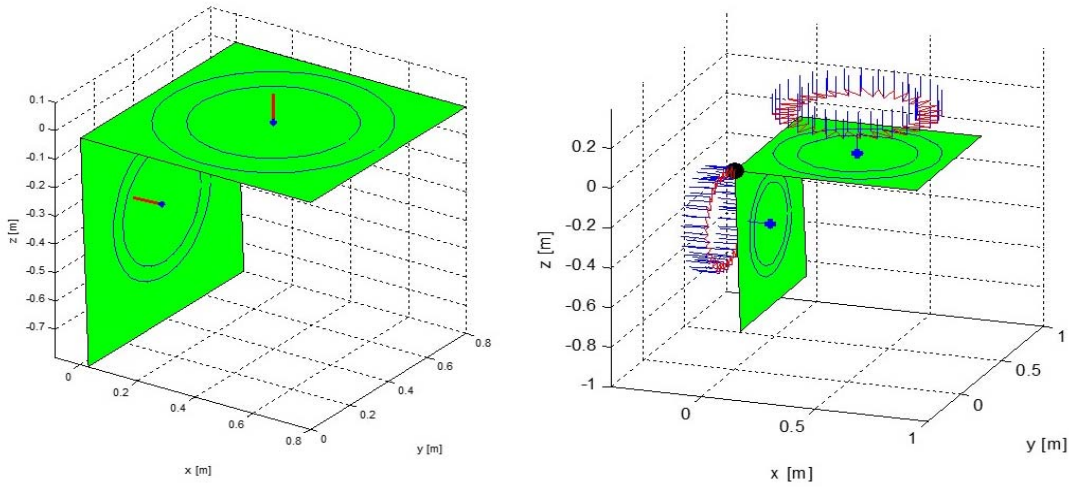


Figure 7. Parametrization of the HLC geometry from data set of Table 2 (left panel) and pre-planned robot motion strategy for inspection of CTQ n. 5 with $\text{angStep} = 0.2 \text{ rad} \gg 11.5^\circ$ (right panel): positions and orientations of robot end-effector are reported in red and blue color, respectively.

- Explicates the whole set of position and orientation of the knots

$$[x, y, z, x_{norm}, y_{norm}, z_{norm}]$$

where x, y, z are robot end-effector coordinates or desired tool positions, $x_{norm}, y_{norm}, z_{norm}$ are components of a unit vector, which is normal to the surface and coming out from it;

- Saves the six vector components within data file.

According to the angStep value, a different set of knots is calculated: for instance, assuming an angular resolution of 30° , a set of 12 knots is inferred to tessellate the whole flange surface (i.e. $360^\circ/30^\circ = 12$). Figure 8 reports this parametrization.

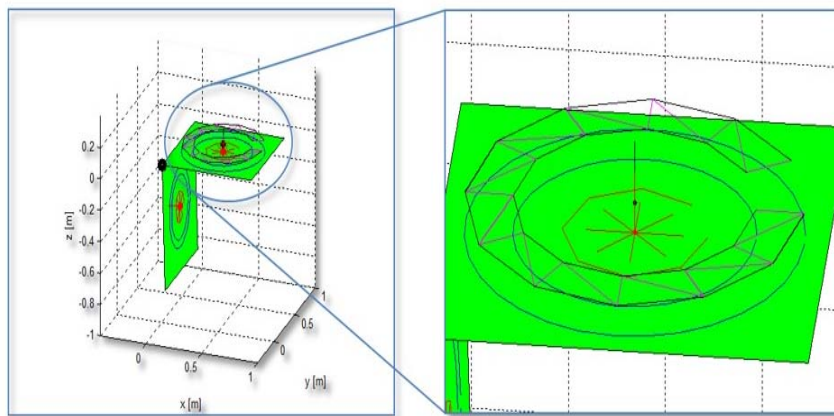


Figure 8. Parameterization of CTQ n. 5 inspection with angStep equal to 30° and surfOffset equal to 50 mm

3.2 Stage 2, *trj2plc*

The second stage, *trj2plc*, aims at:

- ✓ Downloading set of poses to the controller;
- ✓ Feeding robot with one by one pose;
- ✓ Performing robot motion.

Trj2plc is modelled in Simulink environment and interfaced with a program implemented in Fanuc TP programming language within the teach pendant of the robot (par. 3, subpar. 3.3). The model is designed within a desktop Personal Computer (PC), compiled and downloaded - by means of a TCP/IP connection - within an industrial PC. This latter one is connected with robot controller through another TCP/IP protocol. The industrial PC runs Beckhoff TwinCAT 3 system [15], which allows executing compiled models in real-time; code is executed with a 50 ms cycle time, i.e. a sampling frequency of 20 Hz. The industrial PC contains the mapping of robot I/O, the PLC program: this latter one is interfaced with the code - in order to collect data - and with the controller, to manage communication TCP/IP protocol.

The model loads the output collection of poses and pilots the TCP/IP data communication by means of two flags:

- DoneFlag is sent from controller to model (i.e. the industrial PC) when robot is ready to receive new pose slot;
- StartFlag is sent from industrial PC to controller as soon as novel pose has been uploaded.

The two flags are asynchronous and mutually locked, so that only a single flag can be activated at the same time and traffic collision is prevented. An overview of the model is reported in Figure 9: the model integrates a move2robot function, managing list of poses and flag transitions.

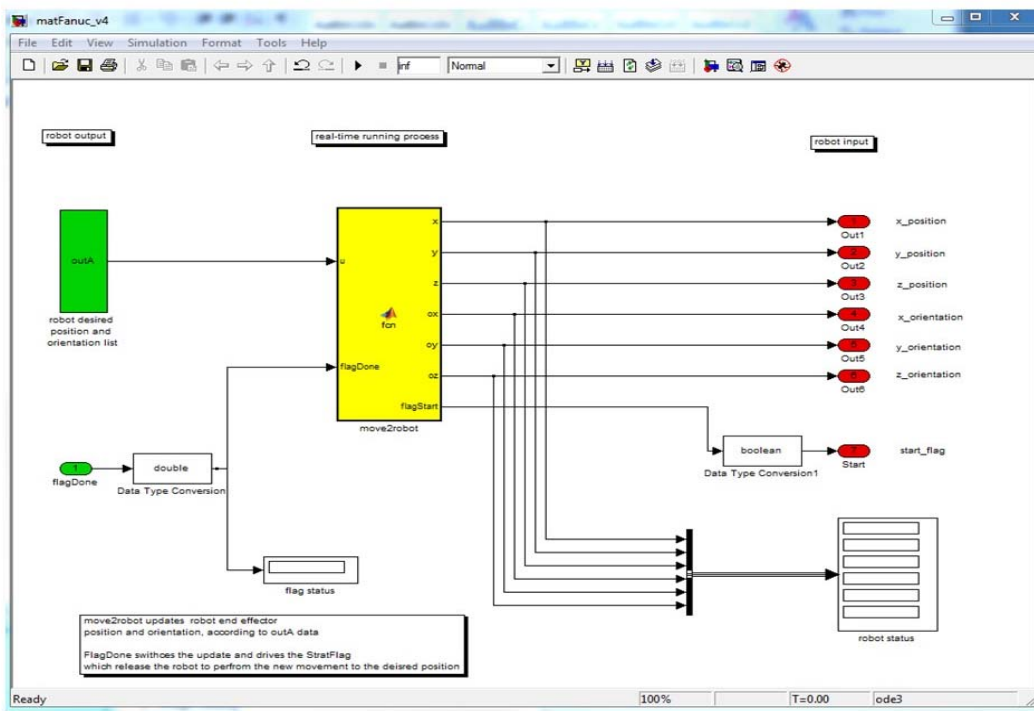


Figure 9. The trj2plc model is implemented through Matlab & Simulink Programming Language, compiled with Industrial PC-based control technology (Beckhoff TwinCAT 3) and interfaced with Fanuc TP program of Robot Arm 30iA Controller

3. 3 Stage 3, plc2scan

StartFlag has been conceived to manage the traffic of data input towards Fanuc robot controller. On robot side, in fact, the TP Program receives the pose or 6 coordinate values (par. 3, subpar. 3.1) and flags to perform robot motion towards the desired poses.

A plc2scan program achieves this task by means of 2 main subroutines (sub):

- Sub1 sets tool and user reference systems - i.e. loads tool and registration parameters - and monitors the input flag;
- Sub2 is called by main program to load poses and assign them to robot position register.

Plc2scan also checks the value of the flag (a), converts (b) and allocates them into register (c). A time delay ($tDelay$) is introduced as further controller parameter: this delay is triggered as soon as a new pose is reached and allows scan device exploring the assigned portion of surface. The default value of $tDelay$ is set at 1.5 s, but this value can be tailored according to rotational speed of the beam and the extension of scanned area. Following this time delay, the TP Program returns positive boolean status of flagDone to trj2plc and communicates that the robot has successfully reached the requested pose (a), the local cycle time has been executed (b) and the robot is ready for a novel pose input (c).

4. Test bed data

Real-time executions of robot trajectories have been accomplished for the inspection of the HLC and validation of CTQ n. 5 (Table 1); trajectory planning - associated to its motion strategy - has been performed with the following test bed data, i.e. values of parameters:

- $angStep = 0.2 \text{ rad} \approx 11.5^\circ$
- $surfOffset = 0.1 \text{ m}$
- $tDelay = 1.5 \text{ s}$

According to this parametrization, a combination of 64 robot poses is prepared ($360^\circ/11.5 \approx 32 \times 2$). Robot trajectories are executed at 50% of maximum speed, resulting in a full flange exploration of less than 2.5 min. Time has been measured with a resolution of $\pm 1 \text{ s}$. An overview of the exploration process is reported in Figure 10.

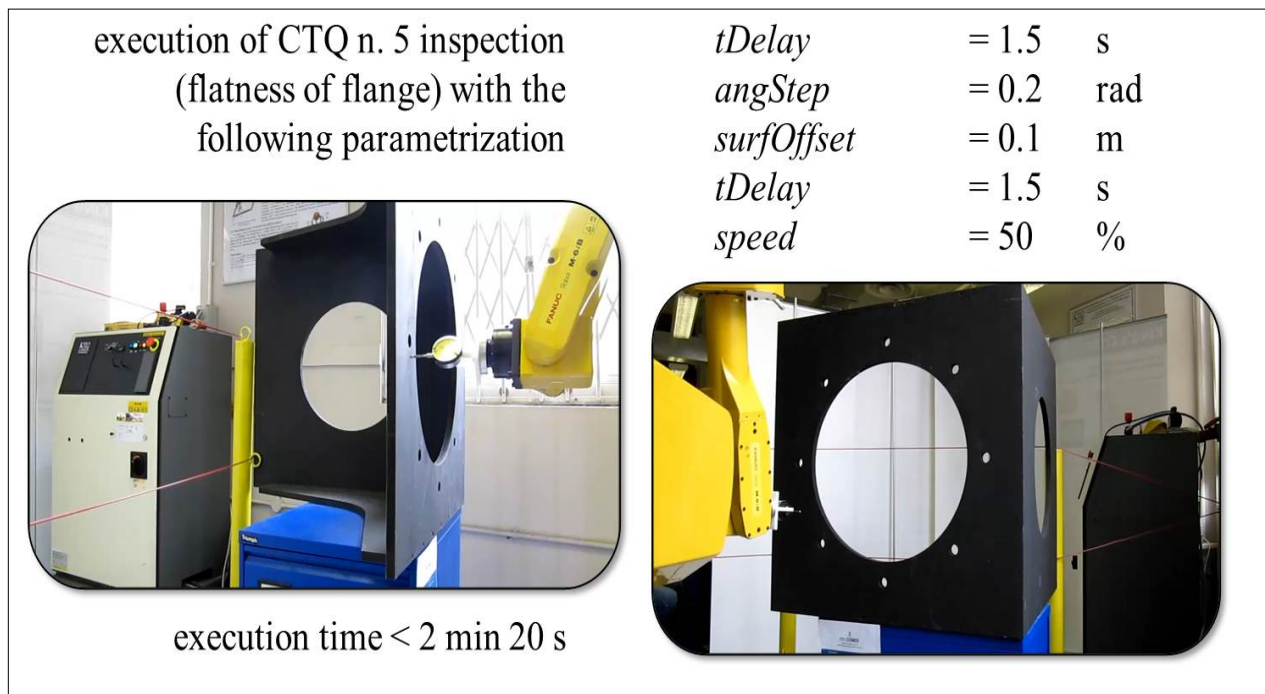


Figure 10. HLC geometric inspection of CTQ n. 5 as performed with Fanuc M-6iB at 50% of its maximum speed

Further tests with differently parameterized trajectories for the geometric inspection of CTQ n. 5 have been performed with different angular resolution, namely 0.05, 0.1, 0.2 and 0.3 rad (2.9° , 5.7° , 11.5° and 17.2° , respectively); these setting yielded to 252, 126, 64 and 42 knots trajectories, respectively. Tests are performed with two values of $tDelay$, namely 0.1 and 1.5 s respectively, at 50% of maximum robot speed.

5. Results

Results are summarized in Table 3: the total exploration time to explore the surface is measured from the first knot to the last. Visualization of the highest density case - i.e. with $angStep = 0.05 \text{ rad} \approx 2.9^\circ$ - is reported in Figure 11.

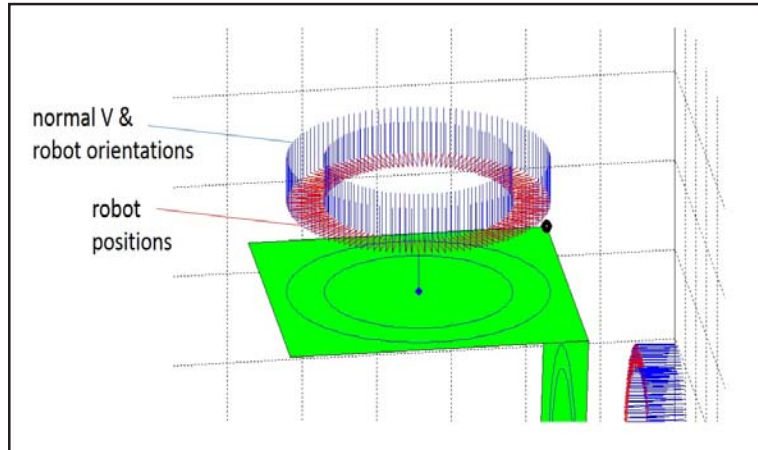


Figure 11. Trajectories parametrization with $angStep$ equal to 0.05 rad ($\approx 2.9^\circ$) and $surfOffset$ equal to 20 mm

Inspections with higher angular resolution - i.e. with lower value of the $angStep$ parameter - require longer execution times; nevertheless, even in the hypothesis of a small scanner FoV, the maximum execution time is less than 15 min.

In order to proof the concept, a Microsoft Kinect XBOX 360 device has been mounted on the robot flange (Figure 12) to explore the HLC: a customized motion strategy has been applied to reconstruct the overall 3D shape of the object and data cloud have been pre-processed with Kinect Fusion Explorer (Microsoft Corp., [16]). 3D object reconstruction has been post-processed with Meshlab software [17]. Data clouds have been acquired with the following parameters set-up:

$$\begin{aligned}
 DT_{min} &= 0.35 \text{ m}; \\
 DT_{max} &= 2.40 \text{ m}; \\
 VM_{ir} &= 197; \\
 VV^m &= 256; \\
 VV^{Rrx} &= 256; \\
 VV^{ry} &= 256; \\
 VV^{Rrz} &= 256.
 \end{aligned}$$

where DT is the depth threshold, VM_{ir} is the volume max integration rate, VV_m is the volume voxel per meter and VV_r is the volume voxel resolution [16]. Figure 12 reports a qualitative comparison between the HLC (right panel) and the 3D reconstruction of the object (left panel).

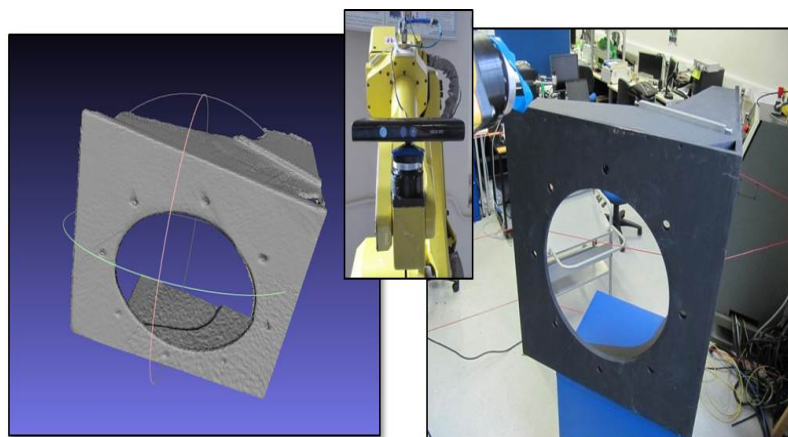


Figure 12. Microsoft Kinect XBOX 360 is mounted on Robot Arm (central panel) to scan the HLC: 3D shapereconstruction (left panel) of the HLC (right panel) is obtained through Kinect Fusion Explorer pre-processing and Meshlab Software post-processing (details in par. 4)

6. Discussion & Conclusion

A real-time and self-adaptive architecture for the geometric inspection of wind turbine hubs has been presented. The architecture is based on the self-planning of robot trajectories (which are implemented from the geometry of the object), the definition of Critical-To-Quality parameters and motion strategy associated with those CTQs.

The inspection has been structured and implemented in three stages for the exploration of re-scaled hub model. An initial registration process, between the robot and the component to be inspected, is needed; registration is based on touching the object with a dial test indicator on three points of the component. Clearly, for this class of geometric inspection, the parameters listed are strictly associated with the type of design and measurement and the performed equipment, however other equipment could be integrated with the appropriate modifications. Moreover, this work has focused on one particular aspect of the wind turbine geometric inspection, namely the inspection of the hub, but it can be easily extend to the quality test of all wind turbine mechanical components.

From the software and hardware viewpoints, the proposed technique combines a desktop computer, an industrial PC running Beckhoff TwinCAT 3 system and a Fanuc M-6iB robot arm, which is connected through a TCP/IP protocol. This set-up can be integrated with other automatic assembly procedure aimed at self-adaptive manufacturing of wind turbine hubs [18-20].

<i>angStep</i>		<i>knots</i>	<i>exploration time</i>	
			<i>tDelay [s]</i>	
			0.1	1.5
<i>[rad]</i>	<i>[deg]</i>	<i>number</i>	<i>[min],[s]</i>	
0.05	2.86	252	5.41	11.37
0.1	5.73	126	2.52	5.50
0.2	11.46	64	1.32	2.58
0.3	17.19	42	1.03	2.01

Table 3. Experimental results performed at 50% of maximum speed of the robot arm

Compared with other metrological techniques, the approach of this work allows re-using robotic devices - which are commonly present in the industrial environment - to perform geometric inspection, rather than purchasing specific devices, like measuring arms or Gantry Machines [6,9]. The literature reports diverse CAD-based methodologies for the automatic trajectory planning of robots, which envisage definition of primitives and optimal trajectories [21-23]; however, main focus of these studies is not on geometric inspection, rather on uniformly distribution of coloured materials on free-form surfaces, as it is the case of automotive spray paintings [22,24]; some methodologies embed image processing modules [23,25] or usage of optical and barrier sensors [23] to infer the object shape, instead of extracting information from the component design. Moreover, in such painting applications, the main purpose relies on preserving a constant paint thickness [21,22], and execution time. To this aim, models of paint gun [21-23,26,27] and paint deposition rate profile can be embedded within the trajectories planner, instead of the optical properties of the scanner, as it is the case of this work.

Although the dissimilar fields of application, further work may compare results obtained with techniques which take inspiration from these methodologies.

7. Funding

The research leading to these results has received funding from the European Commission's Seventh Framework Program (FP7-NMP-2009-SMALL-3, NMP-2009-3.2-2), project COSMOS, Grant No: 246371-2.C.

References

- [1] Herbert, Joselin, GM. (2007). A review of wind energy technologies. *Renewable and Sustainable Energy reviews*. 11: 1117-1145.
- [2] Ezio, CS. (1998). Exploitation of wind as an energy source to meet the worlds electricity demand. *Wind Eng*. 74-76. 375-387.
- [3] Yao, F. (2011). Theory, Design and Applications. *In: Handbook of Renewable Energy Technology*. World Scientific Publishing Co. Pte. Ltd, 3-20.
- [4] Saidur, R. (2010). A review on global wind energy policy. *Renewable and sustainable Energy reviews*. 14. 1744-1762.
- [5] Sharpe, M. (2009). Robotic Fabrication of Wind Turbine Power Generators. Fanuc Robotics.
- [6] Zeiss, Carl AG, Zeiss MMZ G gantry machine. Online Referencing, www.metrology.zeiss.com (accessed 6 February 2014).
- [7] Nikon metrology, NV. (2014). High-Accuracy Gantry CMM. Online Referencing, www.nikonmetrology.com (accessed 6 February).
- [8] FARO Technologies UK Ltd. Laser scanner. Online Referencing, www.faro.com (accessed 6 February 2014).
- [9] Nikon metrology NV. MCA II Articulated arms Portable productivity. Online Referencing, www.nikonmetrology.com (accessed 06 February 2014).
- [10] Vukašinovid, N., Kolšek, T., Duhovnik, J. (2007). Case Study- surface reconstruction from point clouds for prosthesis production. *Journal of Engineering Design*; 18 (5), 475-488.
- [11] Brosed, FJ, Aguilar, JJ., Guillomia, D., Santolaria, J. (2011). 3D Geometrical Inspection of Complex Geometry Parts Using a Novel Laser Triangulation Sensor and a Robot. *Sensors*. 11, 90-110.
- [12] Marin, JAG. (2010). New concepts in automation and robotic technology for surface engineering. Master Thesis, University of Stuttgart.
- [13] Fanuc Robotics Inc. M-6iB Series. Online Referencing, www.fanucrobotics.co.uk (accessed 06 February 2014).
- [14] Secco, EL., Visioli, A., Magenes, G. (2004). Minimum jerk motion planning for a prosthetic finger, *Journal of Robotics System*, 21 (7), 361-368.
- [15] Beckhoff GmbH. Beckhoff. (TwinCAT 3). Online Referencing, www.beckhoff.de (accessed 01 February 2013).
- [16] Microsoft. Kinect Fusion Explorer. Online Referencing, <https://msdn.microsoft.com/en-us/library/dn188670.aspx> [accessed 08 April 2015].
- [17] Meshlab. Download V1.3.3. Online Referencing, <http://sourceforge.net/projects/meshlab/files/meshlab/MeshLab%20v1.3.3/> [accessed 08 April 2015].
- [18] Deters, C., Lam, HK., Secco, EL., Würdemann, HA., Althoefer, K. (2014). Accurate Bolt Tightening using Model-Free Fuzzy Control for Wind Turbine Hub Bearing Assembly. *IEEE Transactions on Control Systems Technology (In press)*.
- [19] Deters, C., Secco, EL., Würdemann, HA., Lam, HK., Seneviratne, LD., Althoefer, K. (2013). Model-free Fuzzy Tightening Control for Bolt/Nut Joint Connections of Wind Turbine Hubs. *In: IEEE International Conference on Robotics and Automation (ICRA)*, Karlsruhe, Germany, 6-10 May, 270-276.
- [20] Lam, HK., Li, H., Deters, C., Secco, EL., Würdemann HA., Althoefer, K. (2014). Control Design for Interval Type-2 Fuzzy. Systems Under Imperfect Premise Matching. *IEEE Transactions on Industrial Electronics* 61 (2), 956-968.
- [21] Chen, H., Xi, N., Sheng, W., Song, M., Chen, Y. (2002). CAD-based automated robot trajectory planning for spray painting of free-form surfaces. *Industrial Robot: An International Journal* 29 (5), 426-433.
- [22] Chen, H., Sheng, W., Xi, N., Song, M., Chen, Y. (2012). Automated Robot Trajectory Planning for Spray Painting of Free-Form Surfaces in Automotive Manufacturing. *In: IEEE International Conference on Robotics and Automation (ICRA)*, St. Paul, USA, 14-18 May, 450-455.
- [23] Gasparetto, A., Vidoni, R., Pillan, D., Saccavini, E. (2012). Automatic Path and Trajectory Planning for Robotic Spray

Painting. Robotik, 211-216.

[24] Pichler, A., Vincze, M., Andersen, H., Madsen, O., Hausler, K. (2013). A Method for Automatic Spray Painting of Unknown Parts. *In: IEEE International Conference on Robotics and Automation (ICRA)*, Karlsruhe, Germany, 6-10 May, 444-449.

[25] Brosted, F.J., Aguilar, J.J., Guillomia, D., Santolaria, J. (2011). 3D Geometrical Inspection of Complex Geometry Parts Using a Novel Laser Triangulation Sensor and a Robot. *Sensors* 11: 90-110.

[26] Meng, F. (2008). Trajectory and spray control planning on unknown D surfaces for industrial spray painting robot. Graduate Thesis & Dissertation, Iowa State University.

[27] Marin, JAG. (2010). New concepts in automation and robotic technology for surface engineering. Master Thesis, Institute for Manufacturing Technologies of Ceramics Components and Composites (IMTCCC), University of Stuttgart.

Author Biographies



Emanuele Lindo Secco received M.Sc. Degree in Mechanical Engineering from University of Padua, Italy, in 1998 and Ph.D. Degree in Bioengineering & Medical Computer Science from University of Pavia, Italy, in 2001. From 2003 to 2014, he worked for Rehabilitation Institute of Chicago (USA), University of Bologna and Eucentre (Italy), Centre for Robotics Research of King's College London (UK). He is Lecturer at Department of Mathematics & Computer Science of Liverpool Hope University (UK). His research is on robotics and sensors.



Christian Deters received the Dipl.-Ing. Degree in Computer Science from Hochschule Bremen, Germany, in 2008 and the M.Sc. degree from King's College London, U.K., in 2009. Dr. Deters obtained a Ph.D. degree at the same Institution in 2014. His research focus is on control, automation, and manufacturing.



Helge A. Würdemann received the Dipl.-Ing. Degree in Electrical Engineering from Leibniz University of Hanover, Germany. In 2006, he was with Auckland University of Technology, New Zealand. In 2007, he was with Loughborough University, U.K., where he carried out a research project. He is currently a Research Associate with the Centre for Robotics Research, Department of Informatics, King's College London, U.K. His Ph.D. project, which he started in late 2008, at King's College London was funded by the Engineering and Physical Sciences Research Council. In November 2011, he joined the research team of Prof. Kaspar Althoefer working on two European Union Seventh Framework Programme projects. His research interests are medical robotics for minimally invasive surgery and self-adaptive control architectures.



Hak-Keung Lam received the B.Eng. (Hons.) and Ph.D. degrees from the Department of Electronic and Information Engineering, The Hong Kong Polytechnic University, Kowloon, Hong Kong, in 1995 and 2000, respectively. Since 2005, he has been with King's College London, U.K., where he was a Lecturer and is currently a Senior Lecturer. He is the co-editor for two edited volumes: *Control of Chaotic Nonlinear Circuits* (World Scientific, 2009) and *Computational Intelligence and Its Applications* (World Scientific, 2012). He is the co-author of the book *Stability Analysis of Fuzzy-Model-Based Control Systems* (Springer, 2011). He is an Associate Editor for the *International Journal of Fuzzy Systems* and serves on the editorial boards of several journals. His current research interests include intelligent control systems and computational intelligence. Dr. Lam is an Associate Editor for the *IEEE Transactions on Fuzzy Systems*.



Kaspar Althoefer received the Dipl.-Ing. Degree in Electronic Engineering from the University of Aachen, Germany, and the Ph.D. degree in Electronic Engineering from King's College London, U.K. He is currently the Head of the Centre of Robotics Research, Department of Informatics, King's College London, U.K., where he is also a Professor of Robotics and Intelligent Systems. He has authored or co-authored more than 200 refereed research papers related to mechatronics, robotics, and intelligent systems.